

# Estimation of the Space Density of Low Surface Brightness Galaxies

F. H. Briggs

Kapteyn Astronomical Institute, Postbus 800, 9700 AV Groningen, The Netherlands

## ABSTRACT

The space density of low surface brightness and tiny gas-rich dwarf galaxies are estimated for two recent catalogs: The Arecibo Survey of Northern Dwarf and Low Surface Brightness Galaxies (Schneider, Thuan, Magri & Wadiak 1990) and The Catalog of Low Surface Brightness Galaxy, List II (Schombert, Bothun, Schneider & McGaugh 1992). The goals are (1) to evaluate the additions to the completeness of the Fisher and Tully (1981a) 10 Mpc Sample and (2) to estimate whether the density of galaxies contained in the new catalogs adds a significant amount of neutral gas mass to the the inventory of HI already identified in the nearby, present-epoch universe. Although tiny dwarf galaxies ( $M_{HI} \lesssim 10^7 M_{\odot}$ ) may be the most abundant type of extragalactic stellar system in the nearby Universe, if the new catalogs are representative, the LSB and dwarf populations they contain make only a small addition ( $\lesssim 10\%$ ) to the total HI content of the local Universe and probably constitute even smaller fractions of its luminous and dynamical mass.

*Subject headings:* ISM – galaxies: luminosity function, mass function – radio lines: galaxies

## 1. Introduction

The goal of this paper is to decide whether there is already evidence that substantial masses of neutral gas have been missed by belonging to such dim galaxies that they have escaped inclusion in the optically selected samples on which HI studies historically have been based. New extensive catalogs of HI observations of dwarf and low surface brightness (LSB) galaxies exist in the literature. Do these new objects make a significant addition to

the integral HI content of the Universe? The question is of central importance to studies of galaxy evolution that monitor neutral gas content as a function of redshift, such as damped Lyman  $\alpha$  absorption-lines in the spectra of quasars (Wolfe et al 1986, Wolfe 1988, Lanzetta 1993, Rao & Briggs 1993, Rao et al 1995).

Since the identification of LSB galaxies is severely hampered by the brightness of the night sky (Arp 1965, Disney 1976, Davies 1993), catalogs that rely on optical selection to specify the numbers of these objects are only now being constructed, through the use of new plate material (Binggeli, Sandage & Tammann 1985, Schombert & Bothun 1988) and plate scanning machines (Irwin et al 1990, Miller & MacGillivray 1994, Impey et al 1994). A substantial majority of the LSB systems is rich in HI (cf. Longmore et al 1982, Schombert et al 1992), implying that large unbiased radio surveys in the 21cm line may ultimately be the most effective means of constraining their space density (Zwaan et al 1997, Schneider 1997).

For the purposes of this paper, the definition of “LSB galaxies” uses the criteria that motivated Schombert and Bothun (1992) to include the galaxies in their catalog, namely that the objects are visible on the new plate material from the POSS II survey plates (Reid et al 1991) with sufficient angular size that they would have been included in an angular-diameter limited sample such as the UGC (Nilson 1973) if they had been of higher surface brightness. The issue is clouded by the fact that some galaxies have low surface brightness disk components, which causes them to satisfy Schombert and Bothun’s definition, and also have a bright, nuclear region that would have caused them to be included in catalogs of normal surface brightness galaxies if they were located nearby, where the nuclear region would subtend a larger angular extent. Thus, there is a danger that a portion of the population of nearby gas-rich dwarf galaxies would be perceived as LSB disk systems when they are detected at higher redshifts. Alternatively, the danger is that distant objects in new catalogs of LSB galaxies are already well represented in the historically important catalogs that have been used to compute luminosity functions and the local luminosity density.

In this paper, the 21 cm line luminosity of optically selected objects is used to parameterize the newly identified population of LSB galaxies in a way that permits their space density to be estimated. The additional contribution of this population to the HI-mass Function of the local Universe can then be compared to the number of systems that comprise the bulk of the entries in large galaxy catalogs such as the CGCG (Zwicky et al 1961) and RC3 (de Vaucouleurs et al 1991). Computation of the integral HI content follows trivially from the HI-mass function and finds immediate application in the interpretation of quasar absorption-line statistics. Due to the HI-richness of the LSB population (Schombert

et al 1992), the HI-mass function also helps to appraise the contribution of the LSBs to the galaxy population as a whole.

The task is simplified by the existence of large catalogs of 21cm line observations. In this paper, the analysis that Briggs and Rao (1993) applied to the Fisher-Tully Catalog (FT, 1981a) is supplemented by (1) the Arecibo Survey of Northern Dwarf and LSB Galaxies (Schneider et al 1990), which relies on the UGC (Nilson 1973) diameter-limited survey to fill in the LSB gaps in the FT Catalog, and (2) the Catalog of Low Surface Brightness Galaxies, List II (Schombert et al 1992), which applies the UGC diameter limit of  $1'$  at the 26.0 mag/square arcsecond isophote of the POSS-II, which is  $\sim 0.8$  mag/square arcsecond fainter than the UGC limiting isophote. Throughout this paper, the Arecibo Survey of Schneider et al (1990) will be referred to as the “DLSB Sample” and the Catalog of Schombert et al (1992) will be called the “P2LSB Sample.” Since these two HI surveys of optically-catalogued galaxies were conducted at similar sensitivity levels with the Arecibo Telescope, they provide large samples, whose selection criteria were designed in a way that complements the earlier FT catalog of HI observations of predominantly bright galaxies. The sensitivity of the Arecibo Telescope ( $\sim 10$  times that of the telescopes used in the FT observations) is necessary to study the dwarf and LSB systems, whose HI fluxes tend to be low due either to their smaller physical size or greater average distances than the higher surface brightness objects that dominate the FT Catalog.

As an introductory overview, note that only 12 galaxies from the DLSB and none of the P2LSB sample are located in the volume used to define the FT 10 Mpc Sample of 355 galaxies detected in HI, once the overlap between the DLSB and FT catalogs is removed. The 12 DLSB galaxies have small HI masses ( $M_{HI} \leq 10^{8.5} M_{\odot}$ ). Despite the fact that the DLSB is drawn from roughly half the solid angle of sky of the FT sample, and the P2LSB is taken from  $\sim 15\%$  of the FT solid angle, the clear implication is that the addition of these new samples cannot add much to the HI content already identified in the population of galaxies described by the FT sample.

In merging the space densities computed for the samples separately, there is a danger of double-counting galaxy populations. For example, although the solid angle,  $\Omega$ , of the P2LSB is much less than the FT, the sensitivity-limited depth,  $d_c$ , of the P2LSB is roughly four times deeper than the FT depth. Since the survey volume is  $\propto d^3 \Omega$ , the identification of  $N$  low surface brightness galaxies in the FT Sample, implies that this same population should have  $\sim 64N \times 0.15 \approx 10N$  representatives in the P2LSB. The space density computed from the larger volume of the P2LSB must not be added to the space density of galaxies determined from the FT Sample unless we are certain that we are adding a population that is not already represented.

As selection of LSB objects is pushed to smaller angular diameters, there is also a danger that, without redshift information, more distant occurrences of familiar populations will be mistaken for a very high space density of small nearby objects. The surface density, number of objects per steradian, will rise by a factor of 8 when the angular diameter limit is halved. Thus, the measurement of redshift is a crucial ingredient to the interpretation of LSB galaxy catalogs.

A description of the analysis of the catalogs fills the bulk of this paper. Section 2 describes the galaxy samples in more detail. Section 3 is an account of the steps in the analysis, leading to the construction of HI-mass functions for the two samples. Section 4 compares the derived HI-mass functions with that of the more familiar “high surface brightness” (HSB) population, and Section 5 attends to the correction of the FT 10 Mpc Sample for incompleteness. Bounds on the space density of LSB galaxies are derived in Section 6 along with an estimate of an LSB HI-mass function for the types of galaxies added by the Catalog of Schombert et al (1992). The comparison between the total HI content contained in the different nearby galaxy populations is made in Section 7. While there are numerous uncertainties in this estimation process, it is unlikely to be in error by a factor of two and represents an attempt to evaluate the contribution of the LSB population relative to the high surface brightness galaxies. A Hubble constant  $H_o = 100 \text{ km s}^{-1} \text{ Mpc}^{-1}$  has been used throughout.

## 2. Properties of the Samples

This section is a review of the properties of the FT, DLSB and P2LSB Samples. Together they form a complementary picture of the HI-rich segment of the nearby galaxy population.

FT constructed their source list for observation in the 21cm line in order to obtain a high degree of completeness for late-type galaxies within  $10 \text{ h}^{-1} \text{ Mpc}$  and with angular diameter  $a \geq 2'$ ; the vast majority of the FT sample is listed in the UGC. The DLSB Sample contains the remainder of the UGC dwarfs and LSB galaxies that fall within the declination range  $-2^\circ$  to  $+38^\circ$  accessible to the Arecibo Telescope, permitting observation of their spectra for HI emission over the redshift range  $-400$  to  $+6500 \text{ km s}^{-1}$  (with a few observed to  $12,000 \text{ km s}^{-1}$ ). The success rate for detection in the DLSB was very high ( $\sim 90\%$ ), which is probably a natural consequence of the morphological selection and the UGC angular diameter constraint  $a \geq 1'$ , which practically guarantees a detectable HI mass at Arecibo. The criteria of Schombert et al. (1990) for selecting the P2LSB Sample from the new POSS II survey plates (Reid et al 1991) specifically excluded galaxies that were

already in the UGC, obtaining a sample that adds to the UGC completeness at the nominal UGC isophotal diameter, as well as creating a new sample with members selected at a more sensitive isophote. The Arecibo observations of the P2LSB routinely covered the velocity range  $-500$  to  $+13,500$   $\text{km s}^{-1}$  with some galaxies observed to  $32,000$   $\text{km s}^{-1}$ . Although Schombert et al (1992) are cautious about the completeness of the P2LSB, they (Schombert & Bothun 1988) use the added sensitivity (to the 26 mag/square arcsecond isophote) of the P2LSB survey to evaluate the incompleteness of the UGC at 11.5%. Furthermore, Schneider et al (1992) use this result to estimate the incompleteness of the DLSB Sample at 14%; Schombert et al (1992) claim to have remedied the incompleteness of the DLSB Sample by augmenting it with the statistics from their deeper P2LSB Samples. Clearly, incompleteness and unknown selection effects are likely sources of error. However, these samples formed the largest available data base for these objects at the time of submission of this paper, and the three catalogs together form a highly complementary description of the late-type galaxy population.

The samples are summarized in Table 1, which lists the number of galaxies in each catalog, the number that were observed in the 21cm line, the number that were detected, and an estimate of the solid angle of the surveys. The specifications cover both the full FT Catalog and the restricted FT “10 Mpc” Sample. The DLSB Sample is divided into two lists, depending on the confidence level that Schneider et al (1990) had in the accuracy of the Arecibo measurement: DLSB-1 contains observations that are free from observational complications, such as possible confusion with a nearby companion or poor spectral baselines which might create a greater than normal source of systematic error, and DLSB-2 lists galaxies for which there *might* be a problem. Schombert et al (1992) divide their catalog into two lists, depending on whether  $a \geq 1'$  (here referred to as P2LSB-1) or  $30'' \leq a < 1'$  (P2LSB-2); the P2LSB-1 and P2LSB-2 together form the P2LSB Sample discussed here, although some properties of the sub-samples will be examined separately. For purposes of the present analysis, the solid angle of sky over which the nominal degree of completeness of the DLSB is expected to apply was estimated to be  $\sim 3.4$  steradians from Schneider et al's Figure 2, by excluding the portion of the sky where Galactic obscuration has clearly influenced the identification of the galaxies. The P2LSB results from inspection of 97 POSS II fields. Each field covers  $6.5^\circ \times 6.5^\circ$ , but edge effects cause incompleteness outside a  $6^\circ \times 6^\circ$  region. The fields are spaced on  $5^\circ$  centers, so that overlap between neighboring fields can occur. However, the sparse coverage of the sky provided by the partially completed POSS II means that the overlap occurred for only a few of the fields from which the P2LSB was drawn (J. Schombert, private communication). For the present application, the independent solid angle per plate was estimated at  $(25 + 36)/2 = 30.5$  square degrees, producing a total of  $\sim 0.9$  steradians for the entire P2LSB Catalog.

The HSB and LSB populations are mixed in the FT and DLSB Samples. One gauge of the HSB content of the FT Sample is the fraction of the sample that is also in the CGCG, which is  $\sim 99\%$  HSB galaxies (Bothun, private communication). Only 41 (13%) of the 302 FT 10 Mpc galaxies in the declination range of the CGCG are not in the CGCG. Since all of the high-mass FT galaxies,  $M_{HI} > 10^9 M_\odot$ , are in the CGCG, we infer that there are no large LSB galaxies in the FT 10 Mpc Sample. (This inference could be in error if some members of the FT Catalog have both bright central regions that cause them to be selected for the CGCG and have extended LSB disks that would cause them to satisfy the P2LSB criteria if they were more distant.) At the low mass end, we have determined that the analytic expression,  $f_L = 0.34 \exp(-M_{HI}/3 \times 10^8 M_\odot)$ , provides a rough description of the fraction of FT galaxies not in the CGCG as a function of  $M_{HI}$  over the range  $10^7$  to  $10^9 M_\odot$ . The DLSB is a mix of classifications: dwarf, irregular, Sd-m, or later. On the other hand, the P2LSB was selected for low surface brightness, but LSB galaxies already in the UGC were omitted from the list. These mixtures in the samples create ambiguities in the analysis that prevent a clean calculation of the space density of a pure LSB population; instead, the samples will be used in this paper to place limits.

Distances to galaxies are determined according to the procedure used by FT: for the majority of the galaxies, the distance,  $d = v_{GC}/H_o$ , is computed using the 21 cm redshift velocity corrected to the reference frame of the Galactic center,  $v_{GC}$ , (de Vaucouleurs et al 1991) and a Hubble constant  $H_o = 100 \text{ km s}^{-1} \text{ Mpc}^{-1}$ . Galaxies within  $6^\circ$  of the core of the Virgo cluster are assigned a distance of 10.7 Mpc, and any remaining galaxies with  $v_{GC} \leq 100 \text{ km s}^{-1}$  are assumed to be members of the Local Group at assigned distances of 1 Mpc. As a result, eighteen galaxies from the DLSB-1, six galaxies from DLSB-2, and none from the P2LSB were assigned the Virgo distance. Only one galaxy (from DLSB-2) was assigned membership of the Local Group. Since only a small fraction of the galaxies in the DLSB and P2LSB lie within 10 Mpc, only small increments to the integral HI mass are made by including the DLSB and P2LSB in the total.

### 3. Analysis of the Samples

The strategy will be to first treat the two surveys as though they sampled independent populations. Then, tests will be applied to determine which segments of the P2LSB and DLSB samples are really the same types of objects already in the FT sample.

The analysis follows the procedures of Briggs & Rao (1993), which they applied to the FT Catalog to derive an HI mass function that compared well with HI-mass functions derived via other routes (Briggs 1990, Rao & Briggs 1993). The method requires that

the sensitivity depth of the survey be determined as a function of neutral gas mass,  $M_{HI}$ . This depth,  $d_c$ , is determined from the observations themselves but is consistent with a theoretical understanding of the sensitivities of radio telescopes. The HI mass  $M_{HI}$  for each galaxy is determined from the measured 21cm line flux and the galaxy’s Hubble distance. The detections are counted in bins of HI mass, and, in order to obtain the HI mass function, the number in each  $M_{HI}$  bin is divided by the volume in which this HI mass would have been detected.

A small simulation was performed to demonstrate how this analysis, which uses the radio detectability of an optically selected sample, can be expected to produce a reasonable estimate of the objects’ space density with high efficiency. The simulation also illustrates how a  $V/V_{max}$  test can be used to check the applicability of the sample.

A galaxy sample was created by randomly populating a cubical volume with galaxies according to a Schechter function with faint end slope  $\alpha = 1.25$ . An optically selected sample was drawn by viewing the contents of the cube from one corner and keeping galaxies satisfying “observational limits” on either magnitude or diameter. Since the samples being discussed in this paper are nominally diameter limited, the sample illustrated in Figure 1 is diameter limited, with  $D \propto L^{0.4}$  according to the Holmberg relation (cf. Holmberg 1975, Peterson, Strom and Strom 1979). This imposes a distance cutoff  $d_c$  for the diameter-limited sample,  $d_c \propto L^{0.4}$ , which is slightly different from the distance cutoff for a magnitude limited sample,  $d_c \propto L^{0.5}$ . As discussed in more detail below, the distance cutoff for detectability in the 21 cm line is  $d_c \sim M_{HI}^{5/12}$ ; coupling this dependence on HI mass with the trend of increasing HI richness toward lower optical luminosities (cf Fisher & Tully 1975, Briggs & Rao 1993),  $M_{HI} \sim L^{0.9}$ , one finds a trend for the HI detection distance cutoff of  $d_c \sim L^{0.375}$ . The similarity of the diameter limited cutoff ( $d_c \propto L^{0.4}$ ) with the HI detectability distance suggests that such an optical, diameter-limited selection will provide a sample with relatively uniform detection rates in the 21cm line across the full span of intrinsic luminosities.

The top panel of Figure 1 shows the distances of 3042 galaxies in a simulated, diameter-limited sample plotted as a function of HI mass. An additional random scatter in HI to optical luminosity ratio was added, with  $\sigma$  of 0.16 dex, to simulate observational errors and allow for variance in the properties of the galaxy population. The solid curves depict 3 choices of sensitivity-limited HI detection distance: the lowest curve indicates a cutoff that detects 35.8% of the optically selected sample, the middle curve detects 74.1%, and the top curve detects 99.8%. The central panel illustrates the  $\langle V/V_{max} \rangle$  ratio (c.f. Schmidt 1968) as a function of  $M_{HI}$  for each of the three HI sensitivities. The lower panel shows the HI mass functions computed from the number of galaxies detected at each of the

sensitivity levels in comparison with the analytic form of the HI mass function computed for mass bins of 0.5 dex (cf Briggs & Rao 1993). The plot shows that a reasonable estimate for the HI mass function can be computed from the detection rate in an optically selected sample, provided the HI observations impose a real sensitivity cutoff in the sample. In other words, the HI observations must be able to detect only a fraction of the sample in order to insure that the survey volume is bounded by the sensitivity of the HI observation. In these cases, it is clear that the two samples that faithfully reproduce the mass function are also the ones that are successful in the  $\langle V/V_{max} \rangle$  test, producing ratios close to 0.5 across the entire range of HI mass. The simulated observation that detects nearly all the diameter-limited sample produces  $\langle V/V_{max} \rangle$  of 0.2 to 0.3 across the mass range and fails to recover the mass function by a factor of 1/2 to 1/3.

The steps involved in evaluating the samples and constructing the mass functions for the DLSB and P2LSB samples are illustrated in Figures 2 through 7. Figure 2 illustrates the survey depths for both Samples by plotting the measured galaxy distances,  $d$ , as a function of  $M_{HI}$ . Smooth curves for the survey depth,  $d_c$ , are plotted in Figure 2; a complete discussion of the choice of functional forms is given by Briggs & Rao (1993). A reasonable description of the survey depth is  $d_c \propto M_{HI}^{5/12}$ , which differs from a simple inverse square law dependence ( $d_c \propto M_{HI}^{1/2}$ ) because galaxies of larger mass rotate faster, spreading their HI flux over a larger velocity width  $\Delta V$  and lowering their detectability. (In brief, the noise level,  $\sigma$ , in a spectrum that has been optimally smoothed to match the HI profile width is  $\sigma \propto 1/\sqrt{(\Delta V)}$ . The minimum detectable HI mass is  $M_{HI} \propto 5\sigma\Delta V d^2$ . A sort of HI Tully-Fisher relation has  $\Delta V \propto M_{HI}^{1/3} \sin i$  for galaxies with inclination  $i$  relative to the plane of the sky, leading to the result that  $d_c \propto M_{HI}^{5/12} \sin^{-1/4} i$ . In fact, enough information exists in the FT catalog to make a first order correction for inclination, which does indeed sharpen the detection boundary (Briggs & Rao 1993). On the other hand, since the inclination and size information is less well determined or not provided for all the samples and the  $\sin^{-1/4} i$  factor is substantially different from unity for a only small fraction of a randomly oriented sample, inclination corrections are not attempted for the analysis of the DLSB and P2LSB Samples.) A still more pessimistic evaluation of the detectability of large masses with  $d_c \propto M_{HI}^{1/3}$ , would lead to flatter mass functions than those illustrated here.

Figure 2 also illustrates the boundaries to the sensitivity of the FT observations and the 10 Mpc limit over which the FT Catalog was intended to be complete. Very few galaxies from either the DLSB or P2LSB fall in the volume where the FT observations could have detected them. The few DLSB galaxies that fall both within 10 Mpc and within the  $d_c$  detection-limited distance cutoff lie close to the  $d_c$  boundary in the mass range  $M_{HI}^{7.2}$  to  $M_{HI}^{8.5} M_{\odot}$ .



Figure 3 shows velocity width  $V_{20}$  of the HI profiles, measured at 20% of maximum, as a function of  $M_{HI}$ . The FT Catalog lists  $V_{20}$ , while, for the DLSB Sample, Schneider et al (1990) list both  $V_{20}$  and  $V_{50}$ , the profile width measured at 50% of maximum. Unfortunately, Schombert et al (1992) tabulate only the  $V_{50}$  widths for the P2LSB. For purposes of comparing the samples, the  $V_{20}$  widths for the P2LSB were estimated by noting that, in the DLSB Sample, the  $V_{50}$  widths are on average  $26 \text{ km s}^{-1}$  larger than  $V_{20}$  (i.e.,  $V_{20} = V_{50} + V_c = V_{50} + 26$ ), although  $V_c$  has scatter over the range from  $\sim 10$  to  $\sim 50 \text{ km s}^{-1}$ . In order to illustrate the effect of this scatter, the estimated  $V_{20}$  for the P2LSB Sample are plotted with error bars that indicate this range. No adjustment for inclination has been applied to either sample.

The curves plotted in Figure 3 were originally derived for the FT sample (Briggs & Rao 1993) and represent a sort of “HI Tully-Fisher Relation” with  $\Delta V = C_0 M_{HI}^{1/3}$ ;  $C_0 = 0.35 \text{ km s}^{-1} M_\odot^{-1/3}$  corresponds to edge-on galaxies, and  $C_0 = 0.08 \text{ km s}^{-1} M_\odot^{-1/3}$  would result from an inclination  $\sim 13^\circ$ . The progression from the higher surface brightness galaxies in the FT sample, through the DLSB to the P2LSB shows a trend of declining velocity width that is especially apparent in the range  $M_{HI} \approx 10^9 M_\odot$ , where there are very few galaxies in the P2LSB that lie close to the  $C_0 = 0.35$  upper bound. This effect indicates that LSB galaxies may rotate more slowly for a given  $M_{HI}$ , which would be consistent with the detailed analysis by Sprayberry et al (1994). Alternatively, it could be an indication that the selection of LSB galaxies biases the sample toward face-on galaxies and that the more highly inclined (edge-on) LSB galaxies are preferentially included in samples of higher surface brightness galaxies, consistent with the statement by Schombert et al (1992) that the survey selection techniques are biased toward face-on systems. Regardless of the cause, the narrower profiles of the P2LSB galaxies make them easier to detect in HI and contribute to making the depth of the Arecibo observations  $\sim 10\%$  greater for the P2LSB than for the DLSB Sample, as can be seen in Figure 2. A second factor that contributes to making  $d_c$  greater for the P2LSB than the DLSB is the improvement in sensitivity of the Arecibo instrumentation with time. The DLSB observations took place in the period 1979 to 1986, and the P2LSB galaxies were observed after 1988. A third consideration is that morphological selection and the angular diameter limit of the UGC have conspired to place the vast majority of the DLSB galaxies above the Arecibo detection limit; the apparent detection boundary of the DLSB may be due to selection rather than due to telescope sensitivity.

The HI-mass functions were estimated following the procedure used previously for the FT catalog (Briggs & Rao 1993). The volume is computed (from the analytic expression for the depth and the estimated solid angle) within which a given  $M_{HI}$  would have been detected. This volume was divided into the number of galaxies with  $d < d_c$  that were

actually detected within an 0.2 dex wide bin centered on that  $M_{HI}$ . In order to plot a quantity that does not depend on the width of the bin, the counts were scaled upward by a factor of five to produce mass functions of “number per Mpc<sup>3</sup> per mass decade.” Since few observations of the DLSB were made for redshifts greater than 8000 km s<sup>-1</sup>, the depth of the DLSB was truncated at 80 Mpc, and no galaxies with greater redshift were included. Similarly, the P2LSB was truncated at a distance of 150 Mpc.

In the following section, the mass function computed from the DLSB sample will not be used in a formal way for the estimation of density of low surface brightness objects, since it is actually a mixture of morphological types and may not actually be a sensitivity limited sample (as discussed above). Instead, the DLSB will be used to add to the completeness of the FT 10 Mpc Sample at the low mass end. On the other hand, the P2LSB sample should have purer morphological selection, and it makes sense to evaluate it using the  $\langle V/V_{max} \rangle$  test. Figure 4 shows  $\langle V/V_{max} \rangle$  plotted in four bins spanning four decades of  $M_{HI}$ . The test is shown for two formulations of  $d_c(M_{HI})$ . The value for  $\langle V/V_{max} \rangle$  is  $0.483 \pm .026$  for the 110 galaxies contained in the detection volume when  $d_c \propto M_{HI}^{5/12}$ , and  $0.489 \pm 0.025$  for 129 galaxies when  $d_c \propto M_{HI}^{1/2}$ .

#### 4. Comparison of the Sample Mass Functions

The HI-mass functions for the FT, DLSB and P2LSB Samples are compared in Figure 5. In the sensitivity limited regime, the survey depth was computed from  $d_c = d_o(M_{HI}/M_\odot)^{5/12}$  Mpc with  $d_o = 0.004, 0.01$  and  $0.011$  for the FT, DLSB and P2LSB, respectively. Error bars, computed from counting statistics, are typically smaller than the symbols, except near the low mass end where there are often only one or two galaxies per bin (see also Figures 4 and 5). Since Figures 2 and 3 indicated no apparent discrepancy in the behavior between the two DLSB-1 and DLSB-2, the two sub-samples have been combined in subsequent calculations of the mass functions. After finding no striking abnormalities in the two P2LSB sub-samples, they too were combined to form a net mass function. As indicated in Table 1, not all members of the P2LSB Sample were observed at Arecibo, so additional correction factors ( $199/155 = 1.28$  for the P2LSB-1 and  $141/101 = 1.40$  for P2LSB-2) have been applied to the space densities based on the assumption that the detection rates would be the same for the unobserved galaxies as for those that were observed. For both the DLSB and P2LSB, a small correction was applied to compensate for the overestimation of the space density of nearby galaxies, due to enhancement by the Local Supercluster; Felton (1977) computes a factor of 2.3 overdensity in luminosity functions based on on samples of nearby galaxies. Galaxies within 15 Mpc were therefore weighted by 1/2 in the counts used

to produce the HI-mass function; as can be seen in Figure 2, this affects only a tiny fraction of the galaxies in these samples.

The histogram for the FT 10 Mpc Sample in Figure 5 has been taken from Briggs and Rao (1993) with a scaling factor of 1/2 to compensate for the overdensity of the Local Supercluster. There are no galaxies in the 10 Mpc Sample with  $M_{HI} > 10^{9.8}M_{\odot}$ , and the HI-mass function plotted for this high mass range is a “maximum envelope mass function” derived from the full FT Catalog in the following manner: the space density was computed for each HI-mass bin as the survey depth was incremented in steps of 5 Mpc. As the cut-off distance was increased from 5 Mpc to  $d_c$ , the peak space density that is obtained for each HI-mass was retained as an upper envelope to the mass function. At the end of the calculation, the maximum density reached in each bin was adopted for plotting in Figure 5. This portion of the FT mass function above  $10^{9.8}M_{\odot}$  has higher uncertainty than the lower mass range for two competing reasons: the nature of the method biases the result toward being too large, while the incompleteness of the FT Catalog at distances beyond 10 Mpc leads to underestimation.

An analytic curve describing the HI-mass function,  $\Theta(M_{HI}/M_{HI}^*)$  (Briggs 1990) is also plotted in Figure 5. This function,

$$\Theta(M_{HI}/M_{HI}^*) = \Theta^*(M_{HI}/M_{HI}^*)^{-0.23} \exp[-(M_{HI}/M_{HI}^*)^{1.11}] \quad (1)$$

where  $\Theta^*$  is  $0.026 \text{ Mpc}^{-3}$  per mass decade, and  $M_{HI}^* = 10^{9.9}M_{\odot}$ , was derived from an expression for the optical luminosity function and an approximate description of the HI richness of spiral and irregular galaxies. The inability of the analytic function to match the FT mass function in the large mass regime may be an indication of incompleteness in the FT survey or it may result from a genuine failure of this simple analytic form to describe the true galaxy population. The analytic curve predicts that 9 galaxies with  $M_{HI} > 10^{9.8}M_{\odot}$  should fall within the volume of the FT 10 Mpc Catalog. An improved fit is obtained by adopting  $\Theta^* = 0.030 \text{ Mpc}^{-3}$  per mass decade and lowering the mass cut-off slightly to  $M_{HI}^* = 10^{9.7}M_{\odot}$ . The large mass regime will eventually be constrained by unbiased radio surveys of large volumes in the 21cm line (cf. Sorar 1994, Spitzak 1996, Zwaan et al 1997).

## 5. Completing the FT 10 Mpc Sample with the DLSB

The 12 galaxies from the DLSB Sample that fall in the volume used for the FT 10 Mpc Sample make a small contribution to the HI-mass function at the low mass end. Figure 6 shows the incremental HI-mass function from these 12 galaxies; the same plot has the HI-mass function derived for the entire DLSB Sample. The heavy solid histogram of Figure

5 shows the modified mass function for the FT 10 Mpc Sample, after the incremental mass function has been added.

## 6. Bounds on the Space Density of LSB Galaxies

The HI-mass functions illustrated in Figure 5 convey the relative space densities of the objects in the catalogs. The difficulty lies in bounding the importance of the low surface brightness portion of the population, which contributes to all three samples. In this section, an approximate mass function for LSB galaxies is derived, after consideration of the limits provided by the Samples.

### 6.1. Upper Bound

An analytic curve (dashed) is drawn in Figure 5 to represent an upper limit to the space density of the LSB population that is already contained in the FT sample. At the low mass end, the curve results from the fraction of the FT galaxies that are missing from the CGCG,  $f_L(M_{HI})\Theta(M_{HI}/M_{HI}^*)$ . The empirically determined cutoff occurs at the same location and with the same shape as that observed for the HI-mass function of irregular galaxies (Rao & Briggs 1993), which was derived from the optical luminosity function for irregulars from Tammann (1986); clearly, the similarity occurs because both curves are related to the same population. For the dashed curve plotted in Figure 5, the cutoff imposed by  $f_L$  is halted at a density of  $1/2000 = 5 \times 10^{-4} \text{Mpc}^{-3}$ , since the volume probed by the FT 10 Mpc Sample is  $\sim 2000 \text{Mpc}^3$ , and nothing can be said about galaxies that are so rare that none are expected in this volume. In fact, the space densities inferred from the P2LSB Samples are sufficiently low that almost no galaxies of the type contained in the P2LSB in the mass range greater than  $10^9 M_\odot$  are expected in the FT volume; at lower masses, both the P2LSB and DLSB populations are compatible with the limit defined by  $f_L$ . Only two galaxies of the variety represented by the DLSB mass function are expected in the FT 10 Mpc volume for  $M_{HI} > 10^9 M_\odot$ , and these could be either dwarfs or LSB galaxies according to the mix in the DLSB Sample.

Given that the above discussion limits the large mass LSB galaxies to be rare, the DLSB Sample mass function itself can be used to form a conservative upper bound. The bound is conservative since the sample is known to be diluted with higher surface brightness objects. At the low mass end, the DLSB mass function lies along the  $f_L\Theta$  curve (Figures 5 and 6), implying that, for small HI-masses, the DLSB Sample may be a good representation

of the objects that are missing from the CGCG. Furthermore, there is only one bin of the HI-mass function for the 12 DLSB galaxies falling in the FT 10 Mpc volume (heavy line with error bars in Figure 6) that lies significantly above the  $f_L\Theta$  curve, suggesting that even if all 12 were LSB galaxies, the curve forms an adequate bound on their space density.

## 6.2. Lower bound

The P2LSB Sample is the only one of the three Samples that has been morphologically selected to be purely low surface brightness galaxies. Therefore, the space densities defined by the HI-mass function (Figures 5 and 7) for the P2LSB form a hard lower limit. Throughout the low mass regime, Figure 7 shows a mass function derived for the P2LSB that does not exceed the dashed curve, which represents the fraction of FT sample missing from the CGCG.

## 6.3. An analytic low surface brightness galaxy HI-mass function

An estimate for the HI-mass function of the low surface brightness population contained in the P2LSB, DLSB and FT Samples is

$$\Phi_{LSB}(M_{HI}/M_{HI}^\dagger) = \Phi_{LSB}^\dagger(M_{HI}/M_{HI}^\dagger)^{-0.25} \exp[-(M_{HI}/M_{HI}^\dagger)^{0.4}] \quad (2)$$

with  $\Phi_{LSB}^\dagger = 0.06 \text{ Mpc}^{-3}$  per mass decade and  $M_{HI}^\dagger = 10^{7.9} M_\odot$ . The function is shown in Figure 7. At the low mass end, this curve includes the DLSB and  $f_L\Theta$  populations. At the large mass end, it traces the mass function defined by the P2LSB Sample. In choosing this form of the curve, we are assuming that the bulk of the low mass galaxies in the DLSB and the FT galaxies not listed in the CGCG are genuine low surface brightness galaxies. At the high mass end, we are assuming that the DLSB sample is heavily diluted by non-LSB objects but that the P2LSB Catalog forms a hard lower bound.

## 7. LSB Contribution to the Total Density

The agreement between the HI-mass function deduced here and the HI-mass function derived earlier by Briggs (1990) from a simple extrapolation of the optical luminosity function is remarkably good, at least down to the mass range  $\sim 10^7 M_\odot$  where the statistics become weak (Figure 5). There is no evidence of a deficit of low mass objects in the range just below  $10^8 M_\odot$  suggested by the analysis of Weinberg et al (1991), and the gently rising

slope of the low mass end indicates that the tiny LSB galaxies at the faint end of the mass function may be the most numerous type of nearby galaxy. The normalization and shape of the HI-mass functions deduced from more detailed considerations of the optical luminosity functions (Rao & Briggs 1993) agree well with the new computation in the mass ranges above  $10^8 M_\odot$ .

The statistics for masses near  $10^6 M_\odot$  are very poor; the LSB galaxies could be the dominant depositories of these tiny quantities of extragalactic HI, although their spatial densities are constrained by surveys in the 21cm line to be no more than a factor  $\sim 10$  above the extrapolation of the mass function from larger masses (Sorar 1994, Zwaan et al 1997). On the other hand, there is, as yet, no evidence that such low mass objects are abundant enough to support even an extrapolation of the HI-mass function to  $M_{HI} = 10^6 M_\odot$ , and observations of dwarf galaxies in the Virgo cluster may indicate a deficit of such low HI-mass objects in that dense environment (Hoffman, Lu & Salpeter 1992).

Although the small field galaxies may outnumber the large ones, they cannot contain much of the HI or luminous mass in galaxies, due to vast importance of the HSB galaxies close to the knee of the mass function. The relative contributions of the FT, DLSB and P2LSB samples to the integral HI content of the local Universe are summarized in Figure 8. The HSB galaxies with  $M_{HI}$  in the range  $10^{8.5}$  to  $10^{10} M_\odot$  dominate the neutral gas content at  $z \approx 0$ . Extrapolating the trends for the DLSB and P2LSB to the poorly determined, low-mass regime around  $10^6 M_\odot$  implies that low-surface-brightness galaxies still provide only a tiny fraction of the total HI. The incompleteness of the FT catalog for galaxies with large  $M_{HI}$  is a concern that is being addressed by on-going HI surveys in the 21 cm line (Sorar 1994). Published observations only constrain the number density of “Malin 1 type” galaxies (Sprayberry et al 1993) to contribute less than  $\sim 10^7 M_\odot \text{ Mpc}^{-3}$  (Briggs 1990), which is comparable to the amount of HI in each 0.2 dex wide bin near the peak at  $M_{HI} = 10^{9.5} M_\odot$ .

The total HI-mass densities, obtained from the integrals over the distributions for each of the three samples in Figure 8, are  $7.28 \times 10^7 h$ ,  $4.5 \times 10^6 h$  and  $2.5 \times 10^6 h M_\odot \text{ Mpc}^{-3}$  for the FT, DLSB and P2LSB respectively. The “corrected” FT 10 Mpc Sample contains  $\rho_{HI} = 7.43 \times 10^7 h M_\odot \text{ Mpc}^{-3}$ , while the analytic expressions using Equation 1 yield  $10.7 \times 10^7 h$  and  $7.7 \times 10^7 h M_\odot \text{ Mpc}^{-3}$  for the original and revised choices of  $\Theta^*$  and  $M_{HI}^*$ , respectively. As fractions of  $\rho_{HI}$ , the DLSB and P2LSB contain 0.065 and 0.034 of the local HI, respectively. The integral of the analytic function for the estimated LSB mass function, Equation 2, yields  $4.9 \times 10^6 h M_\odot \text{ Mpc}^{-3} = 0.052 \rho_{HI}$ . Since the DLSB and P2LSB mass functions form upper and lower bounds to the mass function of the LSB populations in these catalogs, LSB galaxies can contain between  $\sim 3$  and 7% of the HI in nearby galaxies.

Some recognition should be made for the dominant uncertainties: (1) The FT sample draws on galaxies locally in the region which is recognized to have enhanced density. The correction factor (Felton 1977) that was used here has uncertainty. (2) The exact area of sky and degree of completeness of the P2LSB sample (Schombert et al ) are not well quantified. (3) The extent to which variability in the assignment of morphological classification might shuffle previously cataloged galaxies into the LSB bin based on the presence of a extended LSB disk is not well understood. In spite of these uncertainties, the conclusion here is that the new searches at the level of POSS II will not add 15% more HI (i.e. not double the 7% upper limit discussed in the previous paragraph) to the census that is based on complete samples of nearby gas-rich galaxies.

These arguments imply that the HSB galaxies dominate the HI content of the local Universe. Since the LSB galaxies in these DLSB and P2LSB Samples as a class are characterized by large ratios of HI to optical luminosity (Bothun et al 1985), the LSB galaxies should be expected to provide an even smaller fraction of the present epoch luminosity density. Furthermore, the trend seen in Figure 3, indicating that the LSB population rotates more slowly than the HSB galaxies of similar HI-mass, implies that the LSB contribution to “dynamical mass” ( $\propto V_{rot}^2 R$ ) is also a smaller fraction of that already identified with HSB galaxies, since there is no evidence that LSB galaxies have substantially larger gaseous extent,  $R$ , than HSB galaxies of the same HI mass. This conclusion was reached by the detailed study by Longmore et al (1982). There is no evidence that LSB galaxies contain more than a small fraction of the luminous baryonic or the dark matter contents of the Universe. Since the method used in this analysis relies on measurements of HI content and redshifts for the sample members, an LSB population that is free of neutral gas would of course escape inclusion in this analysis entirely.

## 8. Conclusions

Analysis of recent catalogs containing substantial numbers of low surface brightness galaxies shows that the currently catalogued low surface brightness population does not add significantly to the HI content of the local Universe, although their tiniest members could still be the most numerous type of nearby galaxy. Since as a rule the LSB galaxies are relatively rich in neutral gas compared to the high surface brightness population, it is unlikely that these LSBs contribute significantly to the luminosity density or dynamical mass density of the local universe. The effect of lowering the detection threshold by  $\sim 0.8$  magnitudes from the old POSS to the POSS II, appears to add less than  $\sim 3\%$  to the integrated HI content of the Universe. At this rate, lowering the sensitivity to 28 magnitudes

per square arcsecond would only raise the integral HI content by another  $\lesssim 8\%$ . In fact, if a significantly larger number of large gas-rich objects existed, it would already have been identified in a variety of HI surveys (Fisher & Tully 1981b, Briggs 1990, Weinberg et al 1991).

The bulk of the neutral gas content of the local Universe is bound into the larger, HSB galaxies in quantities typically  $M_{HI} \sim 10^{8.5}$  to  $10^{10} M_{\odot}$ , consistent with the computation of the Rao and Briggs (1993), which relates the present HI content to the significantly larger HI densities that are measured by the analysis of QSO absorption lines at high redshifts (cf Lanzetta 1993, Wolfe 1988, Rao et al 1995).

In the time since these results in this paper were submitted for publication, several related studies have been presented in literature. Davies et al (1994) found that giant LSB galaxies are at least an order of magnitude less common than their normal-surface-brightness counterparts, a conclusion consistent with that of Briggs (1990) as well as the mass functions in Figure 7 of this paper. McGaugh et al (1995) concluded that LSB galaxies comprise more than 1/2 the general galaxy population, while McGaugh (1996) finds that LSB galaxies contribute 10-30% of the total luminosity density. Unlike the the analysis presented in this paper, these studies did not make use of redshifts, instead basing the analysis on the surface density of objects on the sky. It is also likely that the P2LSB galaxies are extreme cases of LSB galaxies, so that basing a volume density estimate on them alone will underestimate the total number density that would be obtained if the extreme and intermediate LSB populations were combined (cf. McGaugh 1996). On the other hand, to reiterate the principal conclusion of this paper, pushing down the low surface brightness limits has not produced a big increment in the recognized mass content of the local Universe.

Greg Bothun and Stacy McGaugh have contributed enlightening discussions to the development of this analysis; their comments are greatly appreciated. The author is also grateful to James Schombert and Otto Richter for providing computer files containing the Low Surface Brightness Galaxy Catalog and the Huchtmeier-Richter Catalog of HI Observations of Galaxies, respectively, and to Sheflynn Sherer for assistance with data entry and compilation. This research has made use of the NASA/IPAC Extragalactic Database (NED), which is operated by the Jet Propulsion Laboratory, Caltech, under contract with the National Aeronautics And Space Administration. This work has been supported by NSF Grant AST 91-19930 and NSF Grant AST 88-2222.



## REFERENCES

- Arp, H. 1965, *ApJ*, 142, 402
- Binggeli, B., Sandage, A., & Tammann, G. 1985, *AJ*, 90, 1681
- Bothun, G.D., Beers, T.C., Mould, J.R., & Huchra, J.P. 1985, *AJ*, 90, 2487.
- Briggs, F.H. 1990, *AJ*, 100, 999
- Briggs, F.H., & Rao, S. 1993, *ApJ*, 417, 494
- Davies, J.I. 1993, in *The Environment and Evolution of Galaxies*, ed. J.M. Shull & H.A. Thronson, (Kluwer Academic Publishers: The Netherlands), 105
- de Vaucouleurs, G., de Vaucouleurs, A., Corwin, H.C., Buta, R.J., Paturel, G., & Fougue, P. 1991, *Third Reference Catalog of Bright Galaxies*, (Springer, New York)
- Davies, J.I., Disney, M.J., Phillipps, S., Boyle, B.J., & Couch, W.J. 1994, *MNRAS*, 269, 349
- Dekel, A., & Silk, J. 1986, *ApJ*, 303, 39
- Disney, M.J. 1976, *Nature*, 263, 573
- Felton, J.E. 1977, *AJ*, 82, 861
- Fisher, J. R., & Tully, R. B. 1975, *A&A*, 44, 151
- Fisher, J. R., & Tully, R. B. 1981a, *ApJS*, 47, 139 (FT)
- Fisher, J. R., & Tully, R. B. 1981b, *ApJ*, 243, L23
- Hoffman, G.L., Lu, N.Y., & Salpeter, E.E. 1992, *AJ*, 104, 2086
- Holmberg, E. 1975, in *Galaxies and the Universe*, eds. A. Sandage, M. Sandage and J. Kristian, (University of Chicago Press, Chicago), 151
- Impey, C.D., Sprayberry, D., Irwin, M.J., & Bothun, G.D. 1996, *ApJS*, 105, 209
- Irwin, M.J., Davies, J.I., Disney, M.J., & Phillipps, S. 1990, *MNRAS*, 245, 289
- Lanzetta, K.L. 1993, in *The Environment and Evolution of Galaxies*, eds. J.M. Shull & H.A. Thronson, (Kluwer Academic Publishers: The Netherlands), 237
- Longmore, A.J., Hawarden, T.G., Goss, W.M., Mebold, U., & Webster, B.L. 1982, *MNRAS*, 200, 325
- McGaugh, S.S. Bothun, G.D., & Schombert, J.M. 1995, *AJ*, 110, 573
- McGaugh, S.S. 1996, *MNRAS*, 280, 337
- Miller, R.W., MacGillivray, H.T. 1994, *BAAS*, 25, 1292
- Nilson, P. 1973, *Uppsala General Catalog of Galaxies*, (Uppsala Astr. Obs. Ann., Vol 6).

- Peterson, B.M., Strom, S.E., and Strom, K.M. 1979, *AJ*, 84, 735.
- Rao, S., and Briggs, F.H. 1993, *ApJ*, 419, 515
- Rao, S., Turnshek, D.A., and Briggs, F.H. 1995, *ApJ*, 449, 488
- Reid, I.N. et al. 1991, *PASP*, 103, 661
- Schmidt, M. 1968 *ApJ*, 151, 393
- Schombert, J.M., & Bothun, G.D. 1988, *AJ*, 95, 1389.
- Schombert, J.M., Bothun, G.D., Schneider, S.E., & McGaugh, S.S. 1992, *AJ*, 103, 1107
- Schneider, S.E., Thuan, T.X., Magri, C., & Wadiak, J.E. 1990, *ApJS*, 72, 245
- Schneider, S.E. 1997, *PASA*, 14, in press
- Sorar, E. 1994, Ph.D. Thesis, University of Pittsburgh.
- Spitzak, J. 1996, Ph.D. Thesis, University of Massachusetts.
- Sprayberry, D., Impey, C.D., Irwin, M.J., McMahon, R.G., & Bothun, G.D. 1993, *ApJ*, 417, 114
- Sprayberry, D., Bernstein, G.M., Impey, C.D., & Bothun, G.D. 1994, preprint
- Tammann, G.A. 1986, in *Star-Forming Dwarf Galaxies and Related Objects*, ed D. Kunth, T.X. Thuan, & J. Tran Thanh Van (Gif-sur-Yvette: Editions Frontières), 41
- Weinberg, D.H., Szomoru, A., Guhathakurta, P., & van Gorkom, J.H. 1991, *ApJ*, 372, L13
- Wolfe, A.M., Turnshek, D.A., Smith, H.E., & Cohen, R.D. 1986, *ApJS*, 61, 249.
- Wolfe, A.M. 1988, in *QSO Absorption Lines: Probing the Universe*, ed. J.C. Blades, D.A. Turnshek, & C.A. Norman (Cambridge: Cambridge University Press), 297
- Zwaan, M., Briggs, F., & Sprayberry, D. 1997, *PASA*, 14, in press
- Zwicky, F., Herzog, E., Wild, P., Karpowicz, E., & Cowal, C. 1961-1968, *Catalog of Galaxies and Clusters of Galaxies*, (California Institute of Technology, Pasadena), Vols. 1-6 (CGCG).

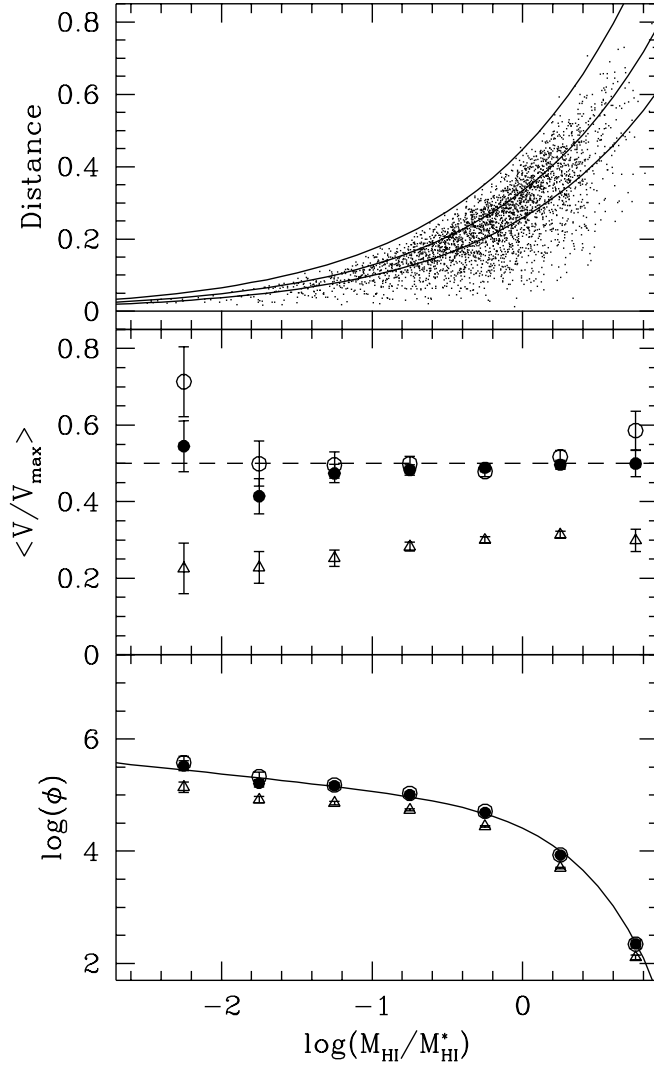


Fig. 1.— Simulation of the method for estimating the HI Mass function. *Top Panel:* Distances of members of a diameter-limited sample of 3042 galaxies plotted as a function of HI-mass. The curves represent sensitivity limited cut-off distance, as a function of HI-mass, imposed by the radio observations in the 21cm line. The simulated observational detection limits include 99.8%, 74.1% and 35.8% of the 3042 galaxies, from upper to lower curves, respectively. *Center Panel:* Results of  $\langle V/V_{max} \rangle$  test for the three simulated detection sensitivities. Open circles for the 99.8% cut, filled circles for 74.1% and triangles for 35.8%. *Bottom Panel* Points (as labeled in the center panel) indicate the mass function derived from the simulated data for the three detection sensitivities. The solid curve is the HI-mass function expected for the parameters used to generate the simulated sample.

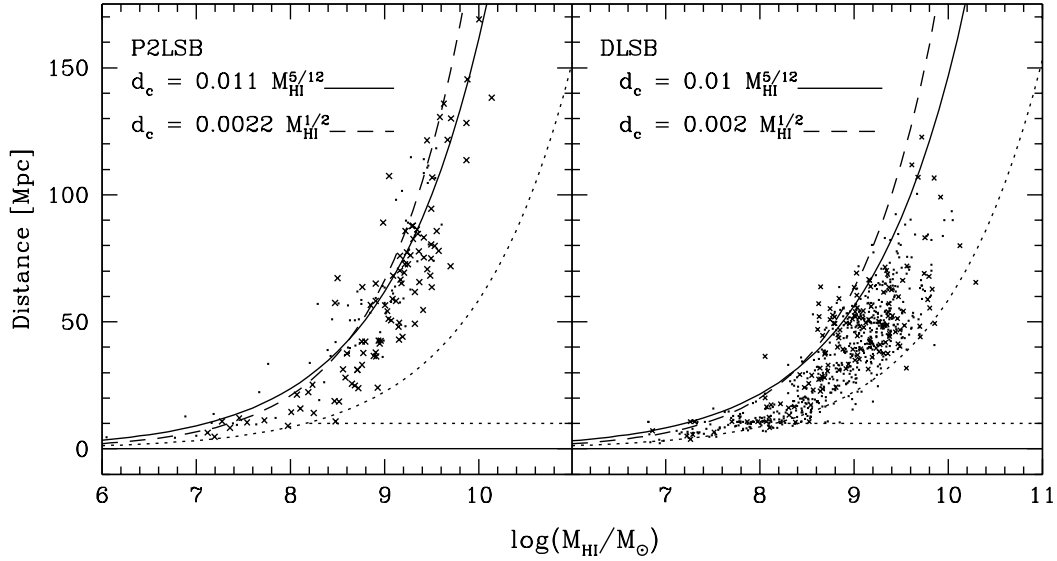


Fig. 2.— Distance as a function of HI mass for the P2LSB Sample *left* and the DLSB Sample *right*. The solid curve indicates the expected sensitivity limit with optimal spectral smoothing ( $d_c \propto M_{HI}^{5/12}$ ) to match the trend of increasing rotation velocity with increasing HI mass. Also shown is  $d_c \propto M_{HI}^{1/2}$  (dashed curve) that would be expected if galaxies of all masses had the same rotation speed. For the DLSB, dots represent galaxies from DLSB-1 and crosses stand for DLSB-2. For the P2LSB Sample, dots represent galaxies with diameters  $30'' < a < 1'$  and crosses represent galaxies with  $a > 1'$ . The dotted curves mark the sensitivity bound of the FT Catalog ( $d_c \propto M_{HI}^{5/12}$ ) and the 10 Mpc depth within which the FT Catalog was designed to be complete.

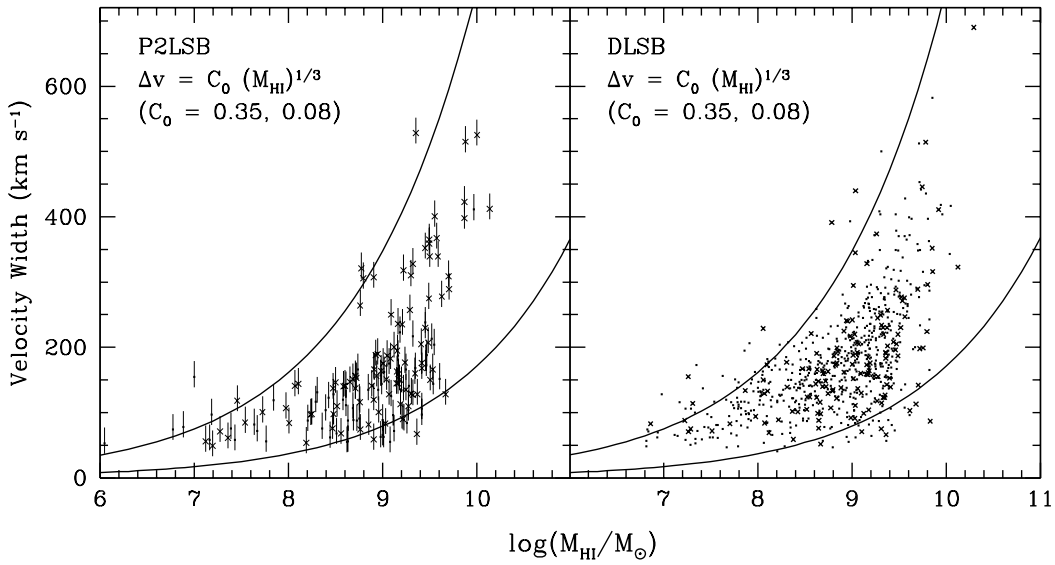


Fig. 3.— Velocity width,  $V_{20}$  as a function of HI mass for the P2LSB Sample, *left* and the DLSB Sample *right*. No correction for inclination has been applied to convert the data from velocity spread to circular rotation velocity  $V_{rot}$ . The upper solid curve forms an estimate of the dependence of  $V_{rot} \approx V_{20}/2 \approx 0.18M_{HI}^{1/3}$  km s<sup>-1</sup>, taken from the analysis (Briggs & Rao 1993) for the Fisher-Tully Catalog (1981a). Error bars in the left panel indicate the uncertainty in adjusting the P2LSB line widths to a system using 20% of maximum (see text). Dots and crosses are assigned as in Figure 2.

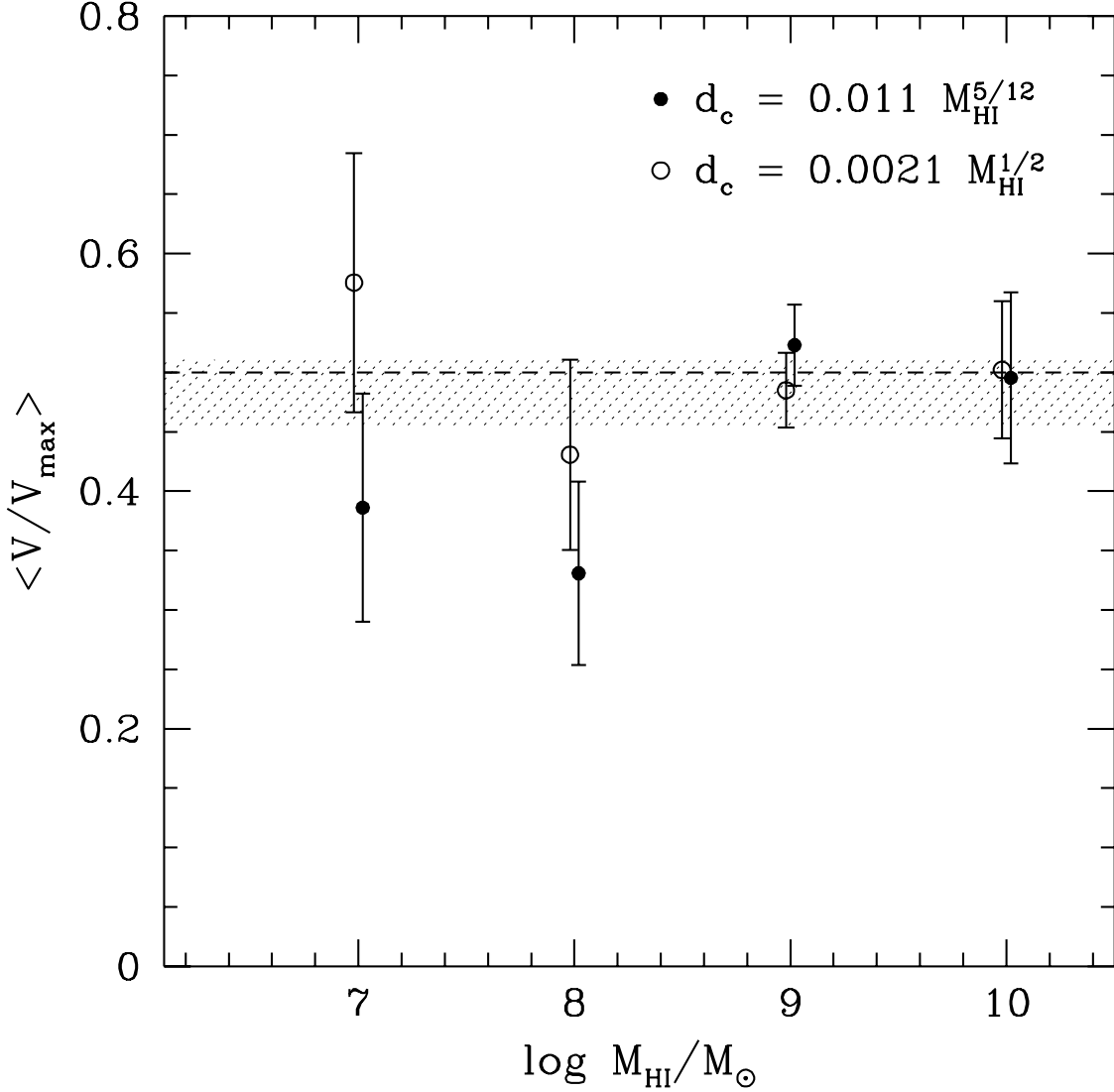


Fig. 4.— Results of the  $\langle V/V_{max} \rangle$  test for the 4 decades of HI mass sampled by the P2LSB Sample. Filled symbols represent a sensitivity limited distance cutoff  $d_c \propto M_{HI}^{5/12}$ ; open circles are drawn for  $d_c \propto M_{HI}^{1/2}$ . The two cases have nearly the same  $\langle V/V_{max} \rangle$  (indicated by the shaded band) for the entire sample analyzed together.

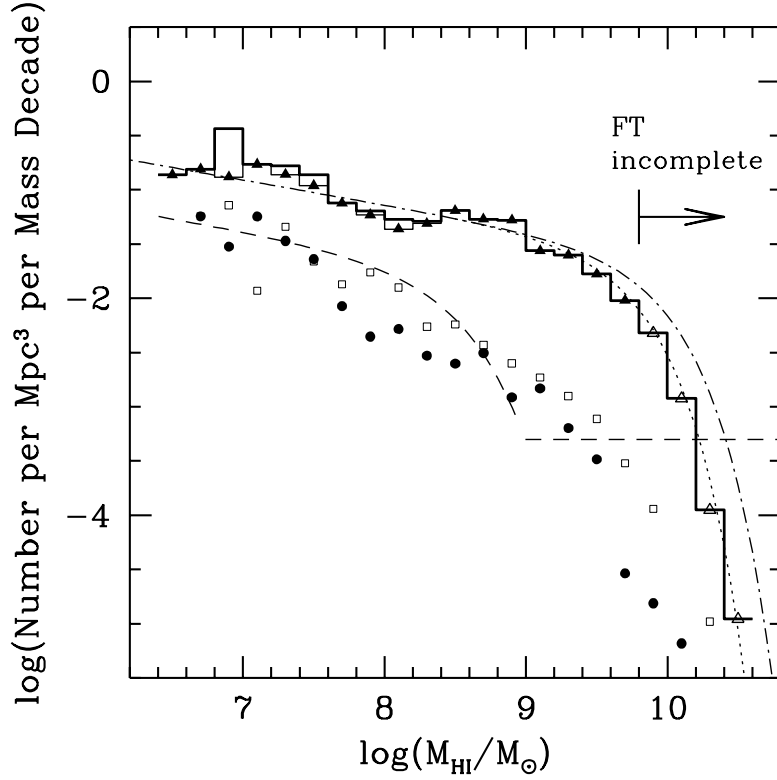


Fig. 5.— The total HI mass function and the mass functions of the FT, DLSB and P2LSB Samples. The total HI mass function, obtained by correcting the FT 10 Mpc Sample, is drawn as a heavy, solid histogram. The P2LSB mass function is marked by filled dots; the DLSB function is marked by open squares; the FT function is marked by triangles. The dot-dash curve results from Equation 1 with  $\Theta^* = 0.026$  and  $M_{HI}^* = 10^{9.9}$ ; the dotted curve adopts  $\Theta^* = 0.030$  and  $M_{HI}^* = 10^{9.7}$ . As described in the text, the dashed curve is an upper bound on the LSB galaxy component of the FT 10 Mpc Sample.

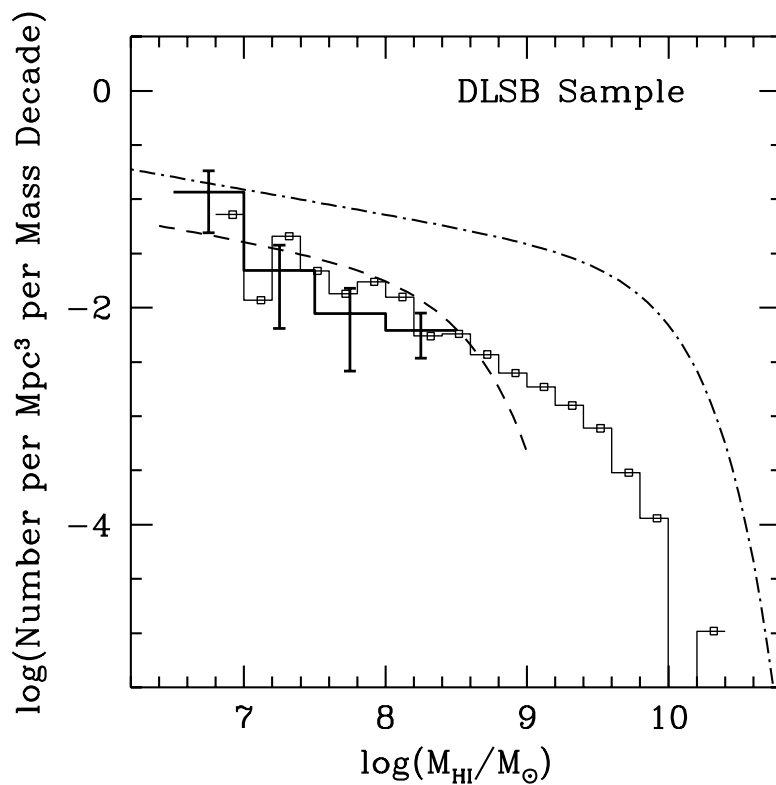


Fig. 6.— HI mass function determined for the DLSB Sample (unfilled squares) The heavy solid histogram indicates the density computed for the 12 DLSB galaxies that fall in the FT 10 Mpc survey volume (bounded in depth by either the FT sensitivity or 10 Mpc, whichever is less). Error bars based on counting statistics are shown for the heavy histogram, which has been binned in half-decades due to the small number of galaxies. The dot-dash and dashed curves are those described in Figure 5.



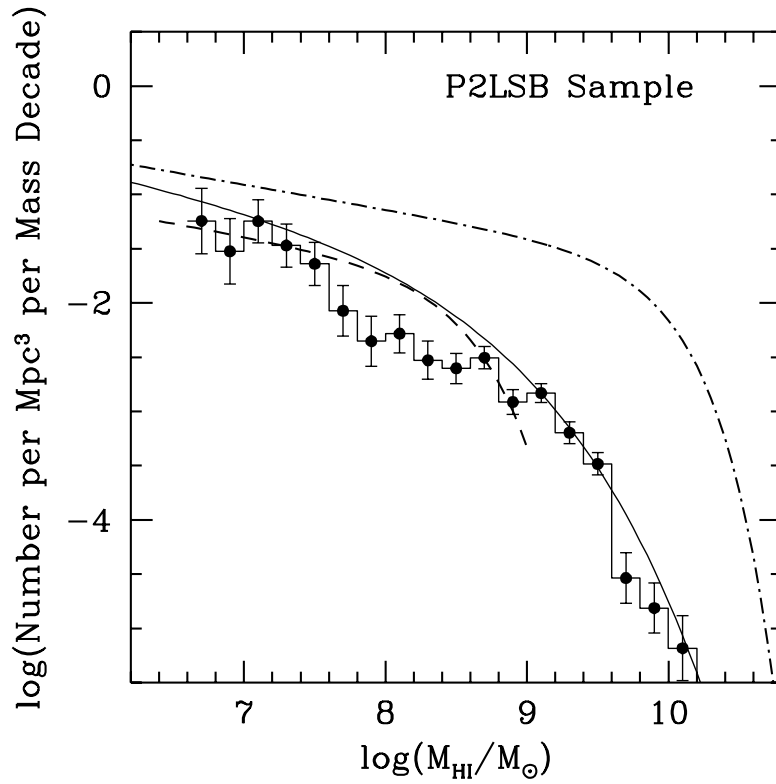


Fig. 7.— HI mass function determined for the P2LSB Sample, indicated by heavy histogram and filled dots. Error bars are based on counting statistics. The smooth solid curve represents the estimated HI-mass function for LSB objects from Equation 2. The dot-dash and dashed curves are those described in Figure 5.

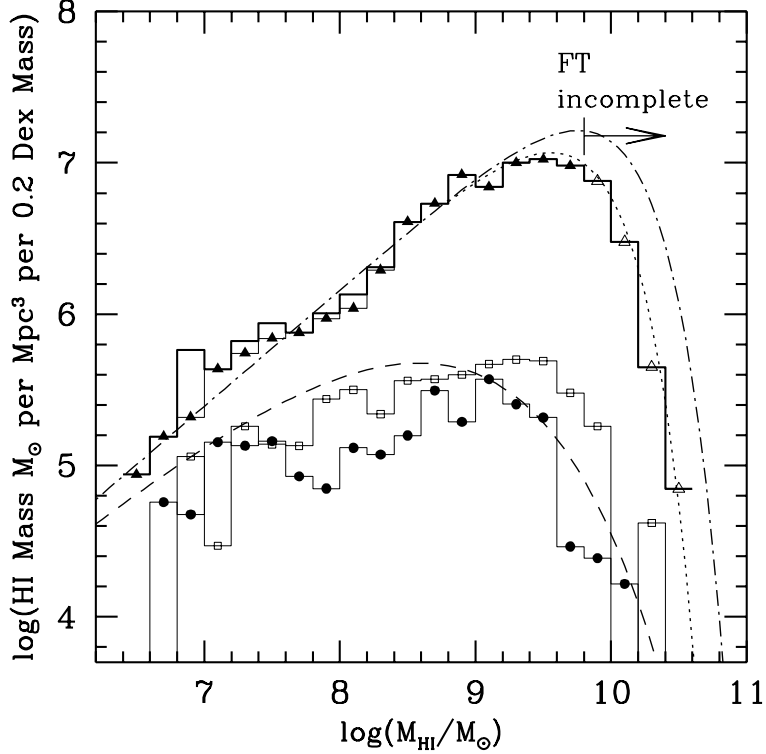


Fig. 8.— The integral HI mass density contained in catalogued populations of galaxies as a function of the HI mass of the host galaxy. The “corrected ” FT Sample is represented as a heavy, solid histogram. The P2LSB Sample is marked by filled dots; the DLSB Sample is marked by open squares; the original FT 10 Mpc Sample is marked by triangles. Smooth curves are drawn to indicate the contents of the analytical models: *dot-dash* integral HI-mass function ( $\Theta^* = 0.026$  and  $M_{HI}^* = 10^{9.9}$ ), *dots* integral HI-mass function ( $\Theta^* = 0.030$  and  $M_{HI}^* = 10^{9.7}$ ), and *dash* estimated LSB HI-mass function.

Table 1. The HI Observations

Sample Name	Total Number of Galaxies	Number Observed	Number Detected	Est. Solid Angle [Sterad]
FT	1720	1720	1153	$\sim 2\pi$
FT 10 Mpc <sup>a</sup>	357	357	343	
DLSB <sup>b</sup>	762	762	709	3.4
DLSB-1	574		574	
DLSB-2	135		135	
P2LSB-1 <sup>c</sup>	199	155	98	0.9
P2LSB-2	141	101	72	

<sup>a</sup>The FT 10 Mpc Sample is a subset of the main FT Catalog

<sup>b</sup>The detections in the DLSB Survey are divided into two subsamples: DLSB-1 and DLSB-2

<sup>c</sup>The detections in the P2LSB Survey are divided into two subsamples, with P2LSB-1 comprising galaxies of angular diameter greater than 1' and P2LSB-2 being less than 1'.